Supplementary material

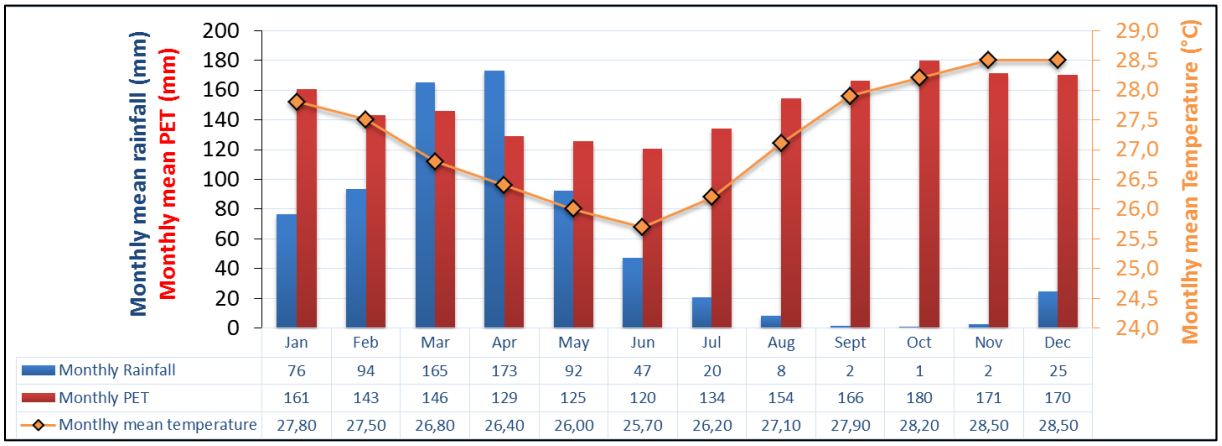

Fig. S1. Monthly values of precipitation, evapotranspiration (PET) and temperature for the Banabuiú watershed. Temperature data extracted from the INMET station n°82586 of Quixeramobim, rainfall and PET data extrapolated using the Thiessen polygon method. PET values calculated from the Hargreaves-Samani method.

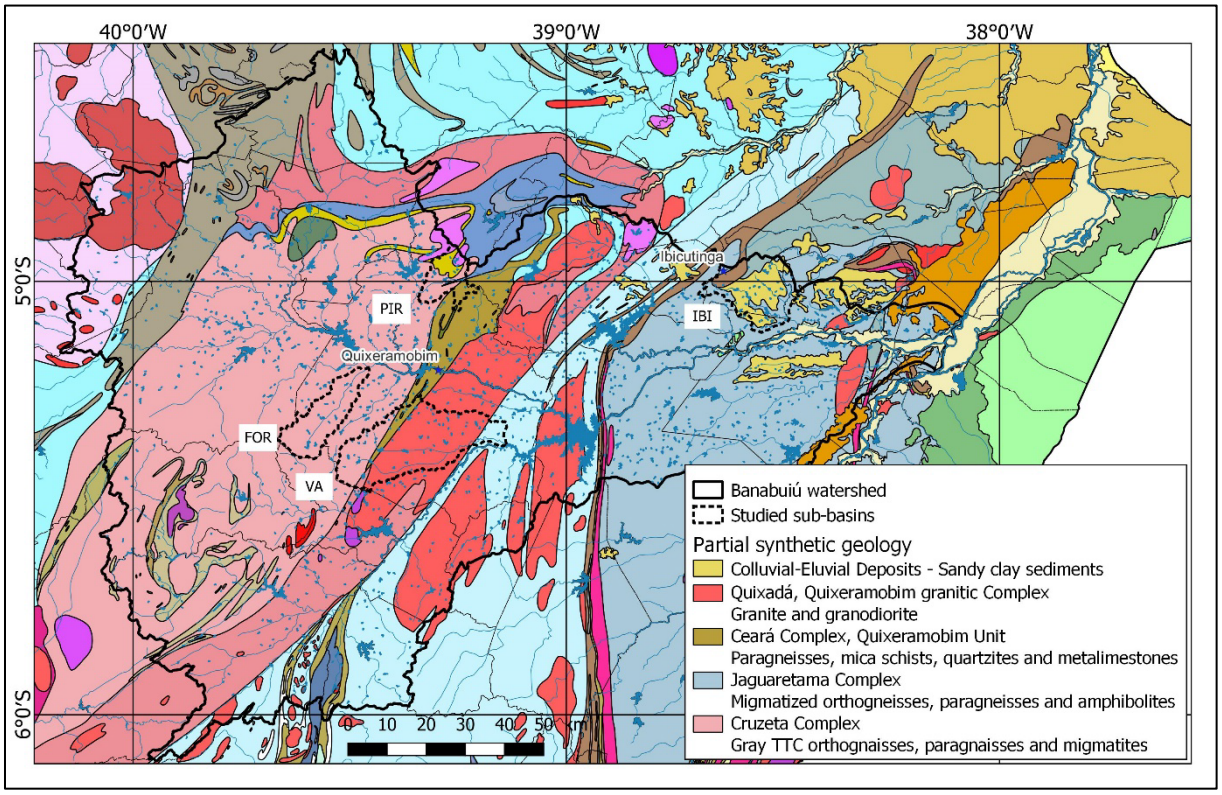

Fig. S2. Geological map of the Banabuiú watershed (1:500.000).

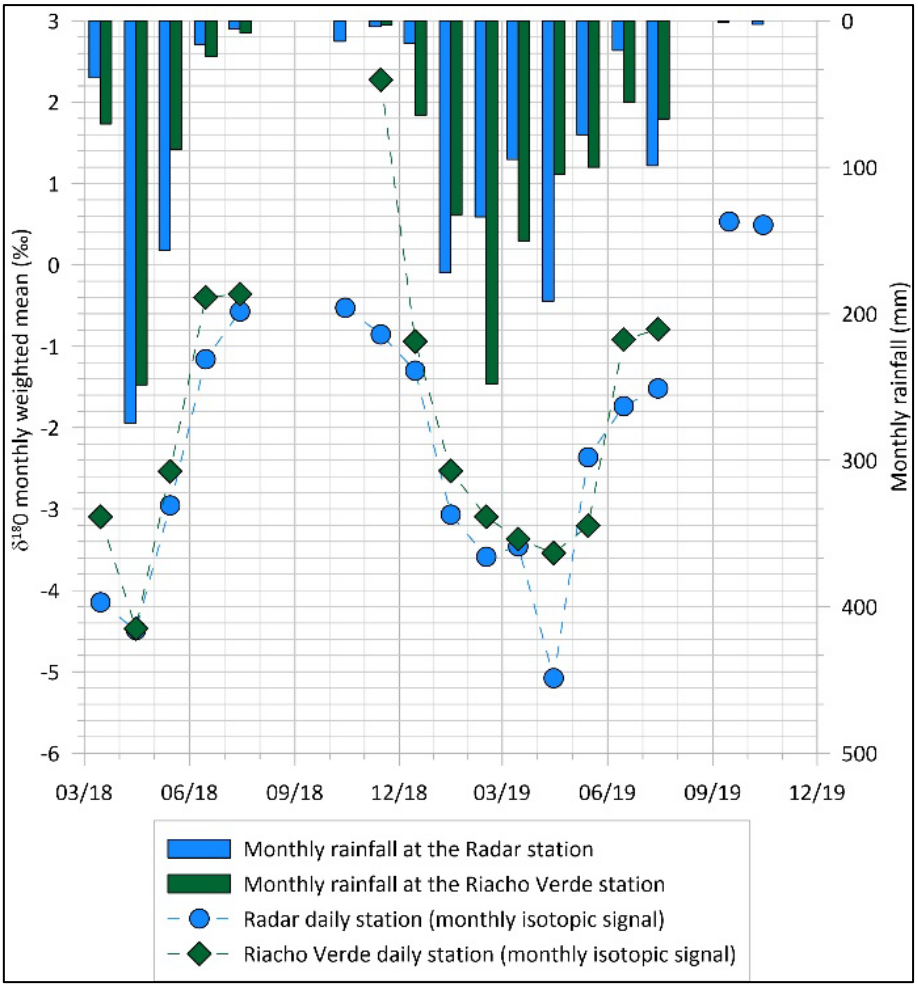

Fig. S3. Monthly isotopic signal calculated by weighting the daily $\delta^{18}O$ with precipitation height.

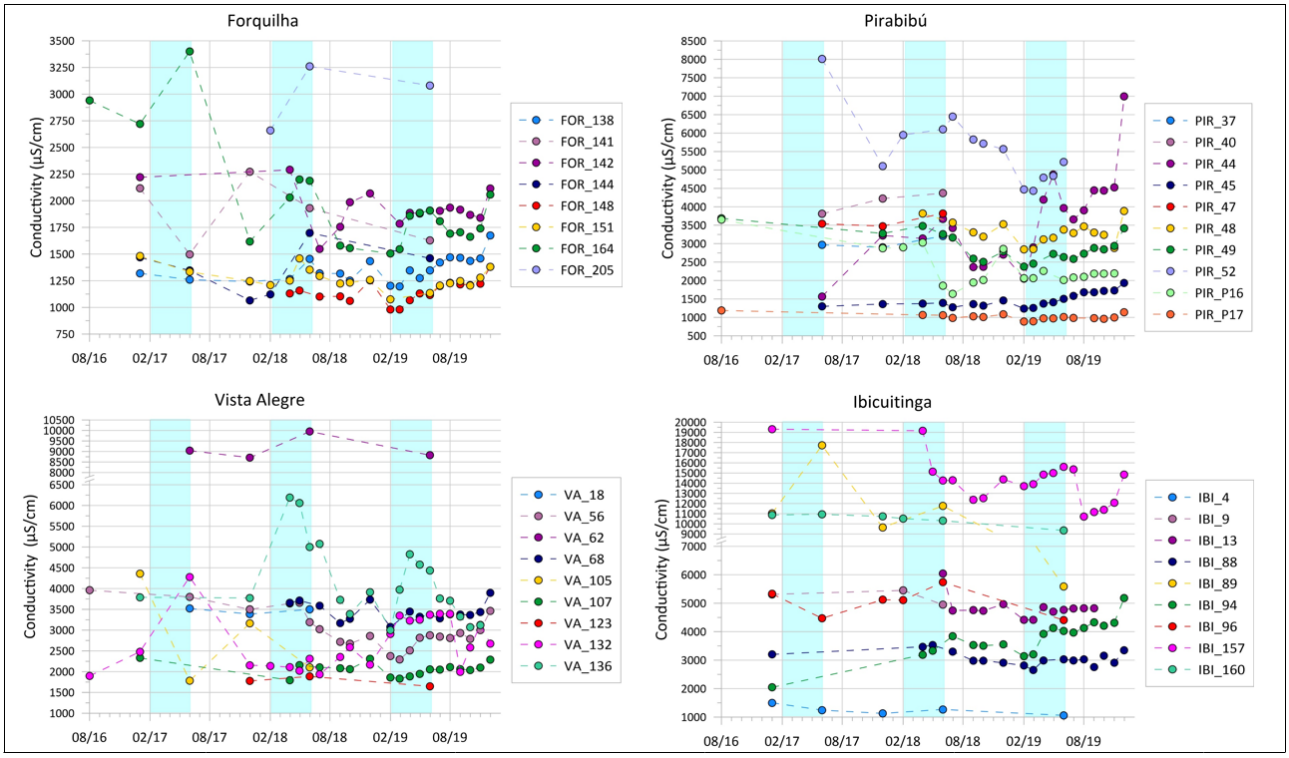

Fig. S4. Monthly EC monitoring of the different sub-basins in the study area between 2016 and 2019.

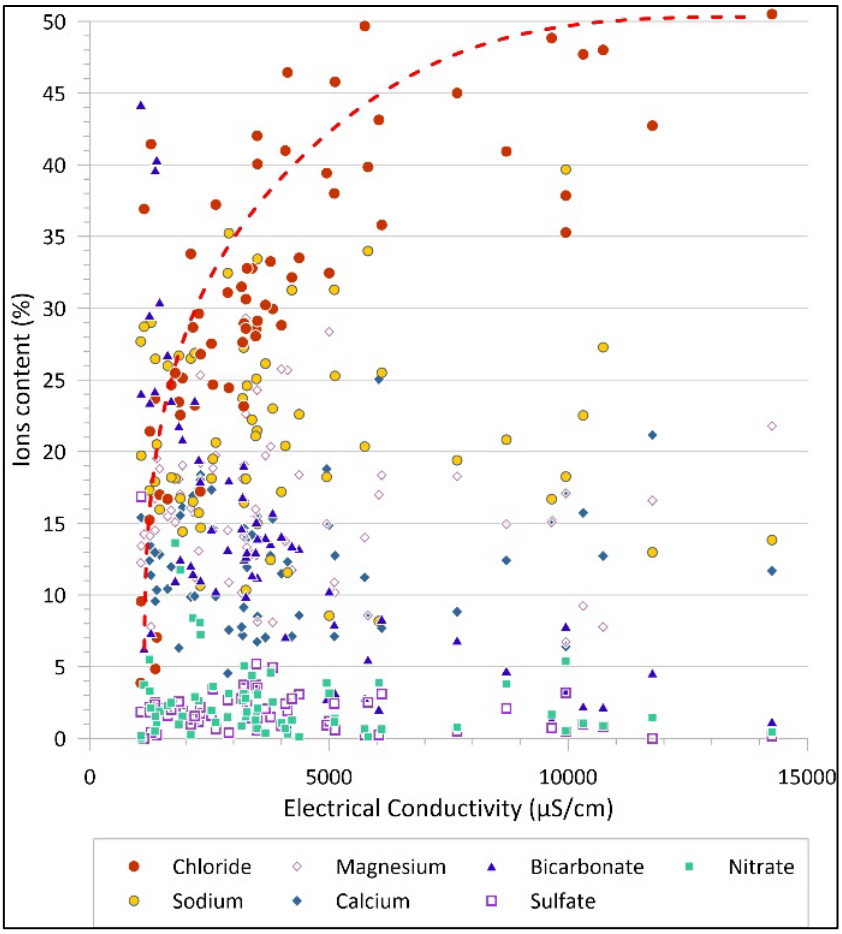

Fig. S5. Proportion of ion contents relative to the total ionic content. The red dashed line represents the augmentation of the chloride proportion with the increasing salinity.

Table S1. Details of the isotopic rainfall station (Kreis et al., 2020).

	Monthly monitoring			**Daily monitoring**	
Station Name	Inmet-Quixeramobim	Algodões-ZéNobre	Vista Alegre	Radar	Riacho Verde
Station ID	-	-	-	766	814
Municipality	Quixeramobim				
Latitude (WGS84)	-5.17	-5.38	-5.34	-5.07	-5.36
Longitude (WGS84)	-39.29	-39.58	-39.40	-39.27	-39.60
Elevation (m)	208	289	206	663	278
Distance to the coast (km)	172	212	195	165	212

Table S2. Assessment of aquifer recharge by the WTF method.

Point	Year	Observation period	Rainfall (mm)	ΔWL (mm)	Δt (a)	Recharge rate (mm a^{-1})	Recharge rate (%)
PIR P14	2017	25/01/2017 to 07/06/2017	561	2600	0.3644	8	1.4
	2018	24/01/2018 to 18/05/2018	494	3340	0.3123	10	2.0
	2019	01/01/2019 to 01/05/2019	340	2070	0.3288	6	1.8
IBI P24	2017	18/12/2016 to 17/06/2017	661	7260	0.4959	22	3.3
	2018	21/01/2018 to 10/07/2018	688	6960	0.4658	21	3.0
	2019	11/12/2018 to 22/05/2019	730	4170	0.4438	13	1.7

Table S3. Analytical results of ^{13}C, ^{14}C and ^{3}H measurements and associated apparent age.

Point	Sampling date	^{14}C	^{14}C	^{13}C	^{3}H
		a^{14}C (pMC)	**Apparent age (a)**	**δ^{13}C (‰)**	**^{3}H (TU)**
FOR P7	2009	126.7 ± 0.5	modern	-16.62 ± 0.1	0.7 ± 0.6
PIR P15	2009	124.4 ± 0.6	modern	-16.84 ± 0.1	1 ± 0.4
VA S. Zuca	2009	119.5 ± 0.5	modern	-15.69 ± 0.1	0.9 ± 0.5
VA 132	2018	110.1 ± 0.5	modern	-16.94 ± 0.1	≤0.7
PIR 52	2018	105.6 ± 0.5	modern	-14.02 ± 0.1	≤0.5
PIR P16	2018	105.3 ± 0.5	modern	-16.73 ± 0.1	0.7 ± 0.3
FOR 144	2018	103.6 ± 0.5	modern	-15.91 ± 0.1	0.6 ± 0.3
FOR 151	2018	98.3 ± 0.5	modern	-15.42 ± 0.1	≤0.7
IBI 160	2018	91.8 ± 0.5	456	-17.20 ± 0.1	≤0.3
IBI 96	2018	73.2 ± 0.6	2327	-17.84 ± 0.1	≤0.4

Table S4. Analytical results of CFC and SF_6 measurements and deduced end-members from the Binary Mixture Model. SF_6 values were corrected by the Excess Air calculated from the relative excess in Neon. *SF_6 contaminated samples (by terrigenous source).

Point	Sampling date	Corrected SF_6	CFC12	CFC11	CFC113	CFC and SF_6 (BMM)	
		pptv	pptv	pptv	pptv	Recent pole (%)	Old pole (%)
PIR 44bis	2019	11.1	550.9	172.6	78.9	-	-
PIR 45	2019	8.3	400.3	133.7	55.5	85	15
FOR 144	2019	6.2	330.2	111.2	42.4	65	35
FOR 151	2019	4.1	368,9	141,9	58,4	50	50
VA 132	2019	4.2	155.6	106.9	29.6	45	55
PIR 52	2019	4.3	133.4	67.8	26.4	35	65
IBI 89	2019	2.0	-	98.8	35.5	40	60
VA 123	2019	3.0	174.5	104.6	46.0	25	75
IBI 96	2019	34.5*	11.0	35.4	13.7	20	80
IBI 152	2019	19.6*	68.5	41.4	13.7	15	85

Table S5. Minor ions and trace elements concentrations. Trace elements whose median concentration is less than 1 µg L^{-1} are not presented.

Element	Unit.	Min.	Max.	Mean	Standard deviation	Median
Si	mg L^{-1}	27.74	61.67	43.98	9.87	44.53
Br	mg L^{-1}	0.21	16.16	2.85	3.92	1.34
Sr	µg L^{-1}	197.01	8933.07	1925.62	2356.05	976.88
Ba	µg L^{-1}	35.65	12922.59	1316.24	2899.63	514.16
B	µg L^{-1}	59.3	723.28	178.43	144.55	142.19
P	µg L^{-1}	23.75	298.24	136.87	75.5	131.28
Mn	µg L^{-1}	0.17	1694.97	197.8	394.8	51.73
Li	µg L^{-1}	9.57	573.02	82.9	127.2	37.85
Fe	µg L^{-1}	3	710.58	119.42	222.06	22.09
Al	µg L^{-1}	3.06	444.37	96.23	144.67	21.41
V	µg L^{-1}	0.61	191.85	44.12	53.03	16.33
Zn	µg L^{-1}	1.05	140.92	19.16	32.34	7.78
U	µg L^{-1}	0.22	64.92	15.37	20.23	6.17
Rb	µg L^{-1}	0.42	203.99	18.86	44.93	4.4
Cu	µg L^{-1}	0.76	16.06	3.59	4.04	2.47
Mo	µg L^{-1}	0.28	26.02	5.06	6.14	2.34
Ni	µg L^{-1}	0.23	14.61	3.08	3.64	1.56
Ti	µg L^{-1}	0.22	52.01	7.03	12.82	1.49
Se	µg L^{-1}	0.11	3.91	1.29	0.94	1.12

Table S6. Cl^-/Br^- molar ratio, Cl^- concentration and electrical conductivity (EC) of the samples.

Borewell	Cl^-/Br^- molar ratio	Cl concentration (mg L^{-1})	EC ($\mu S\ cm^{-1}$)
IBI 96	1217	1517	4408
VA 123	1047	316	1647
VA 62	996	2532	8825
VA 132	935	800	3372
IBI 157	919	6590	15780
FOR 151	900	156	1133
IBI 89	898	1915	5590
FOR 205	890	751	3080
PIR P16	876	416	2015
PIR 52	850	1331	5132
PIR 49	814	603	2603
VA 56	793	521	2875
VA 74	780	384	2180
IBI 4	772	260	1061
IBI 160	771	3386	9350
FOR 144	746	208	1460
FOR 138	690	178	1423
FOR 141	600	317	1628
PIR 45	564	98	1514
PIR P17	255	24	975